Cytogenetic and Genome Research

Original Article

Cytogenet Genome Res 2020;160:238–244
DOI: 10.1159/000508562

Received: November 27, 2019
Accepted: March 26, 2020
Published online: July 14, 2020

Comparative Functional Analysis in vitro of 2 *COL4A5* Splicing Mutations at the Same Site in 2 Unrelated Alport Syndrome Chinese Families

Xing Lv[a] Wei-Qing Wu[a] Jia-Xun Zhang[a] Liu-Fei Miao[a] Bai-Zeng Yu[a] Fang-Fang Chen[a] Ying-Xia Cui[a] Zheng-Kun Xia[b] Zhi-Hong Liu[c] Xiao-Jun Li[a, d]

[a]Institute of Clinical Laboratory Science, Jinling Hospital, Nanjing University School of Medicine, Nanjing, China; [b]Department of Pediatric Nephrology, Jinling Hospital, Nanjing University School of Medicine, Nanjing, China; [c]National Clinical Research Center of Kidney Diseases, Jinling Hospital, Nanjing University School of Medicine, Nanjing, China; [d]State Key Laboratory of Analytical Chemistry for Life Science, Department of Chemistry, Nanjing University, Nanjing, China

Keywords

COL4A5 gene · Minigene · Pre-mRNA splicing · Splice site mutation · X-linked Alport syndrome

Abstract

X-linked Alport syndrome (XLAS) is a common hereditary nephropathy caused by *COL4A5* gene mutations. To date, many splice site mutations have been described but few have been functionally analyzed to verify the exact splicing effects that contribute to disease pathogenesis. Here, we accidentally discovered 2 *COL4A5* gene splicing mutations affecting the same residue (c.2917+1G>A and c.2917+1G>C) in 2 unrelated Chinese families. In vitro minigene assays showed that the 2 mutations produced 3 transcripts in H293T cells: one with a 96-bp deletion in exon 33, one with exon 33 skipping, and one with exon 33–34 skipping. However, fragment analysis results showed that the main splicing effects of the 2 mutations were different, the c.2917+1G>A mutation mainly activated a cryptic donor splice site in exon 33 and resulted in the deletion of 96 bp in exon 33, while the c.2917+1G>C mutation mainly caused exon 33 skipping. Our findings indicate that different nucleotide substitutions at the same residue can cause different splicing effects, which may contribute to the variable phenotype of Alport syndrome.

Alport syndrome (AS) is a common hereditary nephropathy, characterized by hematuria, progressive renal failure, erratically associated with sensorineural hearing loss and ocular defects [Kashtan, 1998; Pirson, 1999]. AS is caused by mutations in *COL4A3*, *COL4A4*, *COL4A5* genes, encoding the α3, α4, α5 chains of type IV collagen, respectively, which is a major constituent of the basement membrane in the kidney, eye, and ear [Kashtan 1999; Hertz et al., 2015; Liu et al., 2017]. X-linked Alport syndrome (XLAS), caused by mutations in the *COL4A5* gene, is the most common AS and accounts for 85% [Feingold et al., 1985; Savige et al., 2013]. The genotype-phenotype correlation in XLAS is relatively well established, and splice site mutations tend to cause a moderate severe phenotype [Bekheirnia et al., 2010; Gross et al., 2012]. More than 1,168 mutations in the *COL4A5* gene have hitherto been identified among which splicing mutations account for about 13–20% [Hertz et al., 2015]. However, functional analyses of most splicing mutations in AS patients have not been performed. Furthermore, comparative transcript analyses of different nucleotide substitutions at the same position have not been reported.

X.L., W.-Q.W., and J.-X.Z. contributed equally to this work.

karger@karger.com
www.karger.com/cgr

Xiao-Jun Li
Institute of Clinical Laboratory Science
Jinling Hospital, Nanjing University School of Medicine
305 Zhongshan East Road, Nanjing, 210002 (China)
xiaojunli62@126.com

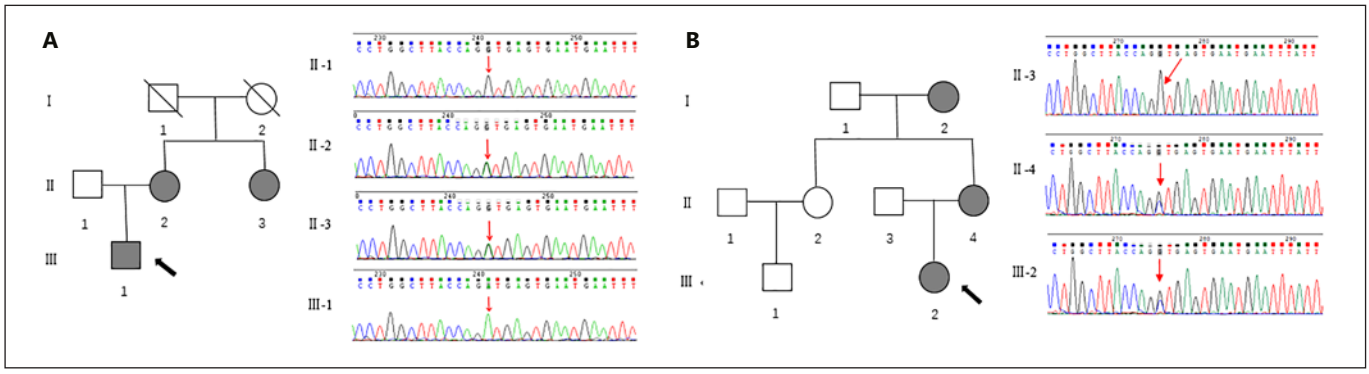

Fig. 1. Pedigree analysis of family 1 (**A**) and 2 (**B**). Gray symbols represent individuals with hematuria or proteinuria, empty symbols indicate normal individuals, probands are denoted with black arrows.

In this study, we identified 2 *COL4A5* splicing mutations affecting the same residue (c.2917+1) in 2 unrelated Chinese AS families. In order to compare the splicing effects of the 2 mutations, we conducted a reporter minigene assay. The results showed that the both splicing mutations produced 3 transcription products; however, the main splicing effects of the mutations were different.

Materials and Methods

Patients

Two probands from 2 unrelated Chinese families were diagnosed with AS based on the classical diagnostic criteria [Gregory et al., 1996]. Renal and skin biopsies were performed by nephrologists, and peripheral blood samples were collected from all participants.

Family 1 is a 3-generation pedigree with 3 affected family members (Fig. 1A). Proband III:1 was detected to have hematuria and proteinuria when he was 11 years old. His mother II:2 and aunt II:3 also presented hematuria and proteinuria, and II:2 progressed to chronic kidney disease (CKD) stage 3 at the age of 32 years. No extrarenal manifestations were observed in any family member. AS diagnosis was based on a kidney biopsy showing characteristic dense layer lamination of the glomerular basement membrane (GBM) and total absence of collagen α3 and α5 chains of GBM.

Proband III:2 of family 2 (Fig. 1B) presented with repeated gross hematuria at the age of 4 years. I:2 and II:4 developed persistent hematuria during their second decade of life. None of the affected members had hearing loss or ocular abnormalities. The proband was diagnosed with AS after a skin biopsy, which revealed partial absence of the α5 chain of collagen IV.

Targeted Next-Generation Sequencing and Sanger Sequencing

The genomic DNA was extracted from peripheral blood of all participants. Targeted capture and next-generation sequencing (NGS) and variants analysis were performed as described before [Liu et al. 2017; Li et al., 2018a, b]. Sanger sequencing was performed on all available family members.

In silico Analysis

The effects of splice site variants on the splicing process were evaluated using Human Splicing Finder (http://www.umd.be/HSF3/HSF.shtml) and NetGene2 (http://www.cbs.dtu.dk/services/NetGene2/) online analysis tools.

In vitro Splicing Assay

We conducted an in vitro minigene assay to analyze the functional effects of the 2 splicing variants. Genomic DNA of the patients or normal controls was amplified using specific primers (*COL4A5*_EX33_F: 5′-AAGAAGTGCAGGATCCATTCATAGAGTACATCCAAGG-3′, *COL4A5*_EX34_R: 5′-CTTTCTCCTGGGATCCACTGCTAAAACTAGAGCCAAA-3′) for exons 33, 34, and flanking intron sequences of the *COL4A5* gene (1,988 bp). The pCAS2 expression vector was used to create minigene constructs, which contained multiple cloning sites between exon A and exon B. The purified PCR products and pCAS2 vector were digested with *Bam*HI restriction enzyme (TaKaRa Biotechnology, China) and ligated together using In-Fusion enzymes (TaKaRa Biotechnology, China). After verifying these sequences by direct sequencing, we obtained a wild-type hybrid minigene (pCAS2-WT) and 2 mutant-type hybrid minigenes (pCAS2-MTA and pCAS2-MTC) (Fig. 2A).

Then, these hybrid minigenes were transfected into H293T cells using Jet Primer (Ploy plus transfection, France) following the manufacturer's instructions. After 24 h, RNA was extracted from each plate of cells using TRIZOL reagent (Invitrogen, CA). cDNA was obtained by reverse transcription of 2 μg RNA samples using PrimScript™ RT Master Mix (TaKaRa Biotechnology, China) and then amplified with pCAS2 plasmid specific primers (pCAS2RT-F: 5′-CTGACCCTGCTGACCCTCCT-3′, pCAS2RT-R: 5′- ATTGGTTGTTGAGTTGGTTGTC -3′) using Premix Taq™ (TaKaRa Biotechnology, China). PCR products were separated by pMD18-T vector and sequenced on an ABI3730xl DNA Sequencer.

In order to quantify all transcripts, fragment analysis was carried out with primer FAM-pCAS2RT-F. GeneScan™1200 LIZ® Size Standard was run as standard substance with FAM-labeled products. Results were analyzed with GeneMarker software.

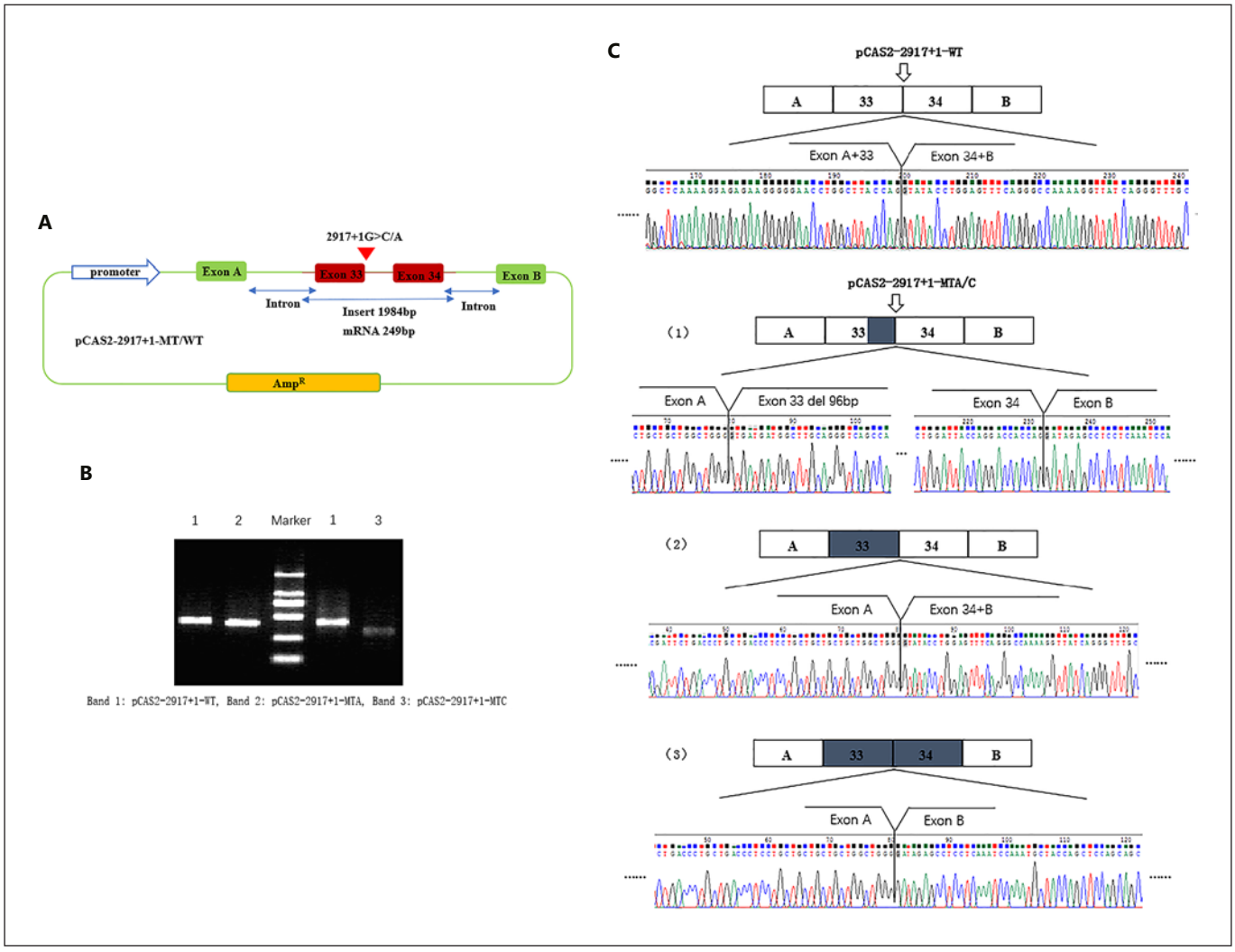

Fig. 2. In vitro splicing analysis of c.2917+1G>A and c.2917+1G>C variants. **A** Schema of the hybrid minigene. The pCAS2 vector contained an Amp resistance gene, a promoter, and 2 exons (exon A and exon B). A 1,984 bp sequence containing exon 33, intron 33, exon 34, and flanking intronic sequences of the *COL4A5* gene was intervened between exon A and exon B, using *Bam*HI and *Mlu*I restriction sites. The position marked by a red triangle was the mutation site. **B**, **C** RT-PCR products of hybrid minigene transcripts. As shown in gel electrophoresis, a comparatively larger transcript was generated from pCAS2–2917+1-WT vector (band 1), while 2 shorter transcripts were generated from pCAS2–2917+1-MTA and pCAS2–2917+1-MTC (band 2 and band 3), which indicated that the 2 mutant vectors had different splicing effects. Sequencing showed that the PCR product of pCAS2–2917+1-WT vector was exon A-exon 33-exon 34-exon B (456 bp), while pCAS2–2917+1-MTA and pCAS2–2917+1-MTC vector had both the 3 same products: (1) exon 33-del96 (360 bp), (2) exon 33 skipping (306 bp), and (3) exon 33 and 34 skipping (207 bp).

Results

Genetic Observations

Targeted NGS revealed 2 splicing variants affecting the same nucleotide site c.2917+1 in intron 33 of the *COL4A5* gene. The proband of family 1 carried a novel heterozygous transition G>A at nucleotide 2917+1 (c.2917+1G>A). This variant was also found in his symptomatic mother and aunt, while it was not found in any asymptomatic family members (Fig. 1A).

The nucleotide transition c.2917+1G>C was identified in the proband of family 2 and was also found in other reports [Knebelmann et al., 1996; Bekheirnia et al., 2010]. Sanger sequencing confirmed this variant segregating with the disease (Fig. 1B).

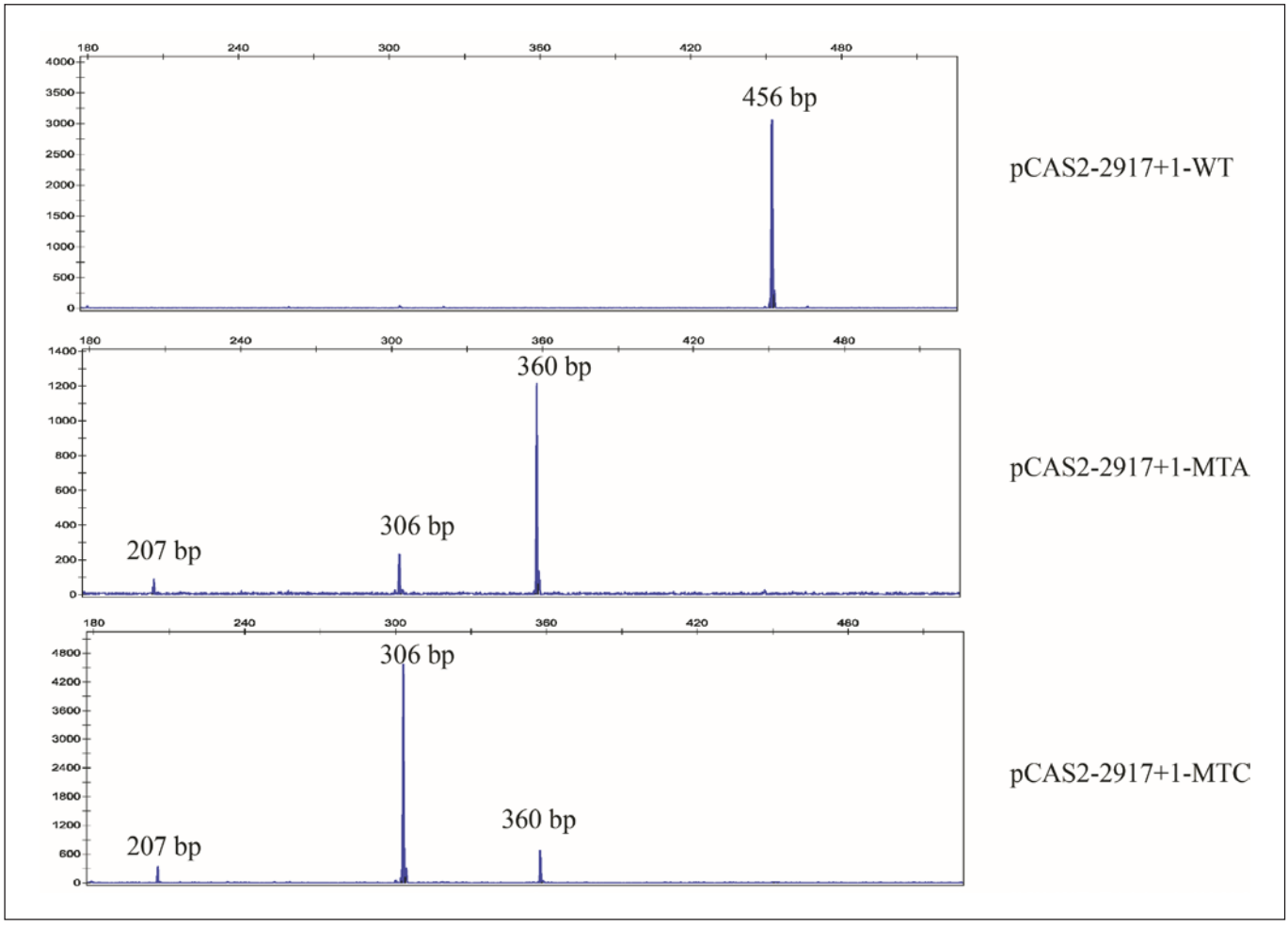

Fig. 3. Fragment analysis of transcripts induced by c.2917+1G>A and c.2917+1G>C variants. pCAS2–2917+1-WT vector had 1 transcript of 456 bp, pCAS2–2917+1-MTA vector had 3 transcripts: 360 bp:306 bp:207 bp at a rate of 16:3:1, while the rate of pCAS2–2917+1-MTC vector was 2:15:1.

In silico Splicing Analysis

The Human Splicing Finder predicted that the c.2917+1G>A and c.2917+1G>C variants in *COL4A5* most probably affected the splicing process by destroying the WT donor site. NetGene2 predicted a 93% drop in confidence that splicing would appear when the variant happened on the position c.2917+1 of the *COL4A5* gene.

In vitro Splicing Analysis

Splicing products of c.2917+1G>A and c.2917+1G>C were analyzed by RT-PCR amplified of extracted RNA as described above. Agarose gel electrophoresis showed that pCAS2-WT plasmid produced a band of the expected 456 bp size, while pCAS2-MTA and pCAS2-MTC plasmids both yielded 2 bands of different lengths and widths (Fig. 2B). Sequencing analysis confirmed that the product of pCAS2-WT was consistent with the reference sequence. In contrast, sequencing of the products of pCAS2-MTA and pCAS2-MTC produced ambiguous results with multiple peaks (results not shown). In order to differentiate the products, purified RT-PCR products were cloned into a pMD18-T vector. Subcloning and sequencing unexpectedly revealed that pCAS2-MTA and pCAS2-MTC both had 3 identical splicing products, one of which caused exon 33 skipping, the other caused exon 33 and 34 skipping, and the last one caused a deletion of 96 nucleotides at the 3′ end of exon 33 (Fig. 2C).

All transcripts were quantified by fragment analysis, and only the transcripts >5% were analyzed. The pCAS2–2917+1-WT vector generated a transcript of 456 bp,

pCAS2–2917+1-MTA vector had 3 transcripts: 360 bp: 306 bp: 207 bp at a ratio 16:3:1, while the rate of pCAS2–2917+1-MTC vector was 2:15:1 (Fig. 3). That is, the major transcript caused by the c.2917+1 G>A variant was a deletion of 96 bp in exon33, while the c.2917+1G>C mutation mainly was responsible for exon 33 skipping.

Discussion

Alport syndrome is caused by mutations in *COL4A3*, *COL4A4,* or *COL4A5* encoding α3–5 chains of type IV collagen. Currently, more than 1,000 *COL4An* gene mutations have been described, and 13–20% of them are splicing mutations [Hertz et al. 2015]. However, most of splice site mutations in AS patients were proven to be pathogenic only by analysis of a variant segregation with the disease at the DNA level, but the exact splicing effects have not been verified in functional studies. Knebelmann et al. [1996] and Bekheirnia et al. [2010] found a c.2917+1G>C mutation, but they did not verify it at the RNA level. In this study, we applied targeted NGS to identified 2 *COL4A5* gene splicing variants affecting the same residue (c.2917+1G>A and c.2917+1G>C) in 2 unrelated Chinese AS families and we confirmed the pathogenicity of the 2 variants using a simple in vitro reporter minigene assay.

The recognition of the splice site is the key step of the pre-mRNA process, and the sequence of the canonical acceptor and donor site is highly conserved. Therefore, any mutations in these canonical sequences might lead to abnormal splicing products. The splicing effect caused by theses mutations includes exon skipping and activation of a cryptic splice site [Hertel, 2008; Anna et al., 2018]. The definite splicing effects may relate to the strength of canonical and cryptic splice sites, exon and intron length, the order of intron removal, the abundance of exonic splice enhancers and silencers, or a RNA secondary structure [Takahara et al., 2002; Tazon-Vega et al., 2007; Habara et al., 2009; Anna et al., 2018]. In our study, the results of the minigene assay showed that both c.2917+1G>A and c.2917+1G>C mutations had 3 functional consequences: 2 of them caused the skipping of 1 or 2 exons, and the third transcript activated a donor cryptic splice site located at position c.2820–2821. Several diverse transcripts can be generated if the splice site is weak and the mutation stimulates the use of a neighboring cryptic splice site, like seen in variants of *CFTR* and *COL5A1* gene [Takahara et al., 2002; Ramalho et al., 2003]. Notably, the major outcome of the c.2917+1G>A mutation was a partial deletion of exon 33, while the major outcome of the c.2917+1G>C mutation was exon 33 skipping. The reason of this difference is unknown, but we speculated that it may be related to a different strength of the splice sites after different nucleotide substitutions. A functional study about *DMD* gene splicing mutations revealed that the same substitution (G>A) at the same +1 position of exon 25 and 45 had different effects. The authors suggested that if the canonical splice site is strong (with high complementarity to the splicesome), the probability for the activation of a cryptic splice site is higher; on the contrary, if the primary splice site is weak, there is a higher probability of exon skipping [Habara et al., 2009]. A quantitative in vitro study suggested that the level of different transcripts might vary with individual genetic differences [Xu et al., 2014]. Altogether, it is difficult to predict the effect of a splicing variant in various genetic diseases, because splice effects occur from the interaction between negative and positive elements. Our results show that different base substitutions may be an influencing factor.

The 2 cases with mutations at the same +1 position in intron 33 of the *COL4A5* gene but differential splicing effects might be considered a good model for exploring the influencing factors of splicing regulation. It is the most direct and effective method for determining the splicing effect of a specific mutation to investigate RNA extracted from mutation-specific expressed tissues or cells from a patient [Anna et al., 2018]; in the case of AS, this is by using the mRNA of the patient's kidney or skin tissue. But in our 2 probands kidney or skin biopsies have been performed several years ago, and we were unable to obtain fresh tissue samples. Some studies extracted RNA from hair follicles of AS patients for transcriptional analysis [Tazon-Vega et al., 2007; Malone et al., 2017]. We also tried to extract RNA from the hair follicles, but unfortunately the purity and concentration of RNA is too low to analyze, probably because abnormal transcription products are unstable in this tissue. In silico analysis tools can be used to predict the effect of splice site variants on the splicing process, while precise transcription products should be verified in functional studies. In vitro minigene assay is an alternative method if the tissues or cells for functional RNA sequencing are not available. Some studies examined the utility of the minigene assay in case of inherited kidney disease by detecting the same abnormal transcription produces by in vivo and in vitro minigene assays [Nozu et al., 2009; Nakanishi et al., 2017].

Patients with XLAS have a variable phenotype-genotype correlation [Jais et al. 2000]. Gross et al. [2012] have previously reported that males with XLAS caused by

splice donor mutations had a relatively severe phenotype. Bekheirnia et al. [2010] showed that affected participants with splice site mutations had a higher risk of developing eye problems and hearing impairment. But most of the reports had not investigated the correlation between phenotype and genotype at the RNA level. The *COL4A5* gene encodes α5 chains of type IV collagen, which include a short 7S domain at the amino terminal end, a long collagenous domain with Gly-X-Y repeats, and a non-collagenous (NC1) domain at the carboxy terminal end [Hudson, 2004]. In our study, minigene analysis revealed 2 different transcription effects, which mainly led to the in-frame deletion of 50 or 32 amino acids in the Gly-X-Y region, respectively. Clinical data showed that none of the 2 family members had progressed to end-stage kidney disease and none had extrarenal manifestations. There was no significant difference in the phenotype between the 2 families. In other words, the difference of the 18 amino acids in in vitro analysis may be not enough to cause significant differences in their clinical phenotypes. Horinouchi et al. [2018] suggested that male XLAS patients with splice site mutations that result in non-truncating splicing abnormalities were associated with a better prognosis versus those that create a premature stop codon. But because of the lack of adult male patients in our study and females and young boys usually having mild phenotypes, the lack of features with the splice site mutations is not unexpected. We need longer follow-up and a larger sample size to determine whether different splicing effects affect the severity of the patients' phenotype.

In summary, this study identified 2 *COL4A5* gene splice site mutations affecting the same position (c.2917+1G>A and c.2917+1G>C) in 2 XLAS families using targeted capture and NGS. We used an in vitro minigene assay to determine the pathogenicity of the 2 mutations, and fragment analysis results showed that c.2917+1 G>A mainly caused a partial deletion (96 bp) of exon 33, while c.2917+1 G>C mainly resulted in exon 33 skipping. This is the first report of a comparative functional analysis of 2 *COL4A5* gene mutations at the same site in XLAS.

Acknowledgement

We thank the patients and their families for participating in this study. This work was supported by a grant from the Science and Technology Program of Jiangsu Province (BL2014072).

Statement of Ethics

All participants signed informed consent forms before participating in the study. This study was approved by Ethics Committee of the Jinling Hospital.

Disclosure Statement

The authors have no conflicts of interest to declare.

References

Anna A, Monika G: Splicing mutations in human genetic disorders: examples, detection, and confirmation. J Appl Genet 59:253–268 (2018).

Bekheirnia MR, Reed B, Gregory MC, McFann K, Shamshirsaz AA, et al: Genotype-phenotype correlation in X-linked Alport syndrome. J Am Soc Nephrol 21:876–883 (2010).

Feingold J, Bois E, Chompret A, Broyer M, Gubler MC, et al: Genetic heterogeneity of Alport syndrome. Kidney Int 27:672–677 (1985).

Gregory MC, Terreros DA, Barker DF, Fain PN, Denison JC, et al: Alport syndrome–clinical phenotypes, incidence, and pathology. Contrib Nephrol 117:1–28 (1996).

Gross O, Licht C, Anders HJ, Hoppe B, Beck B, et al: Early angiotensin-converting enzyme inhibition in Alport syndrome delays renal failure and improves life expectancy. Kidney Int 81:494–501 (2012).

Habara Y, Takeshima Y, Awano H, Okizuka Y, Zhang Z, et al: In vitro splicing analysis showed that availability of a cryptic splice site is not a determinant for alternative splicing patterns caused by +1G→A mutations in introns of the dystrophin gene. J Med Genet 46: 542–577 (2009).

Hertel KJ: Combinatorial control of exon recognition. J Biol Chem 283:1211–1215 (2008).

Hertz JM, Thomassen M, Storey H, Flinter F: Clinical utility gene card for: Alport syndrome – update 2014. Eur J Hum Genet doi:10.1038/ejhg. 2014.254 (2015).

Horinouchi T, Nozu K, Yamamura T, Minamikawa S, Omori T, et al: Detection of splicing abnormalities and genotype-phenotype correlation in X-linked Alport syndrome. J Am Soc Nephrol 29:2244–2254 (2018).

Hudson BG: The molecular basis of Goodpasture and Alport syndromes: beacons for the discovery of the collagen IV family. J Am Soc Nephrol 15:2514–2517 (2004).

Jais JP, Knebelmann B, Giatras I, De Marchi M, Rizzoni G, et al: X-linked Alport syndrome: natural history in 195 families and genotype-phenotype correlations in males. J Am Soc Nephrol 11:649–657 (2000).

Kashtan CE: Alport syndrome and thin glomerular basement membrane disease. J Am Soc Nephrol 9:1736–1750 (1998).

Kashtan CE: Alport syndrome. An inherited disorder of renal, ocular, and cochlear basement membranes. Medicine (Baltimore) 78:338–360 (1999).

Knebelmann B, Breillat C, Forestier L, Arrondel C, Jacassier D, et al: Spectrum of mutations in the *COL4A5* collagen gene in X-linked Alport syndrome. Am J Hum Genet 59:1221–1232 (1996).

Li A, Cui YX, Lv X, Liu JH, Gao EZ, et al: The *COL4A3* and *COL4A4* digenic mutations in cis result in benign familial hematuria in a large chinese family. Cytogenet Genome Res 154:132–136 (2018a).

Li A, Gao EZ, Cui YX, Liu JH, Lv X, et al: Three novel heterozygous *COL4A4* mutations result in three different collagen type IV kidney disease phenotypes. Cytogenet Genome Res 154: 30–36 (2018b).

Liu JH, Wei XX, Li A, Cui YX, Xia XY, et al: Novel mutations in *COL4A3*, *COL4A4*, and *COL4A5* in Chinese patients with Alport Syndrome. PLoS One 12:e0177685 (2017).

Malone AF, Funk SD, Alhamad T, Miner JH: Functional assessment of a novel *COL4A5* splice region variant and immunostaining of plucked hair follicles as an alternative method of diagnosis in X-linked Alport syndrome. Pediatr Nephrol 32:997–1003 (2017).

Nakanishi K, Nozu K, Hiramoto R, Minamikawa S, Yamamura T, et al: A comparison of splicing assays to detect an intronic variant of *OCRL* gene in Lowe syndrome. Eur J Med Genet 60:631–634 (2017).

Nozu K, Iijima K, Kawai K, Nozu Y, Nishida A, et al: In vivo and in vitro splicing assay of *SLC12A1* in an antenatal salt-losing tubulopathy patient with an intronic mutation. Hum Genet 126:533–538 (2009).

Pirson Y: Making the diagnosis of Alport's syndrome. Kidney Int 56:760–775 (1999).

Ramalho AS, Beck S, Penque D, Gonska T, Seydewitz HH, et al. Transcript analysis of the crystic fibrosis splicing sites and suggests a putative role of exonic splicing enhancers. J Med Genet 40:e88 (2003).

Savige J, Gregory M, Gross O, Kashtan C, Ding J, et al: Expert guidelines for the management of Alport syndrome and thin basement membrane nephropathy. J Am Soc Nephrol 24: 364–375 (2013).

Takahara K, Schwarze U, Imamura Y, Hoffman GG, Toriello H, et al: Order of intron removal influences multiple splice outcomes, including a two-exon skip, in a *COL5A1* acceptor-site mutation that results in abnormal pro-alpha1(V) N-propeptides and Ehlers-Danlos syndrome type I. Am J Hum Genet 71: 451–465 (2002).

Tazon-Vega B, Ars E, Burset M, Santin S, Ruiz P, et al: Genetic testing for X-linked Alport syndrome by direct sequencing of *COL4A5* cDNA from hair root RNA samples. Am J Kidney Dis 50:257.e1–14 (2007).

Xu W, Yang X, Hu X, Li S: Fifty-four novel mutations in the *NF1* gene and integrated analyses of the mutations that modulate splicing. Int J Mol Med 34:53–60 (2014).